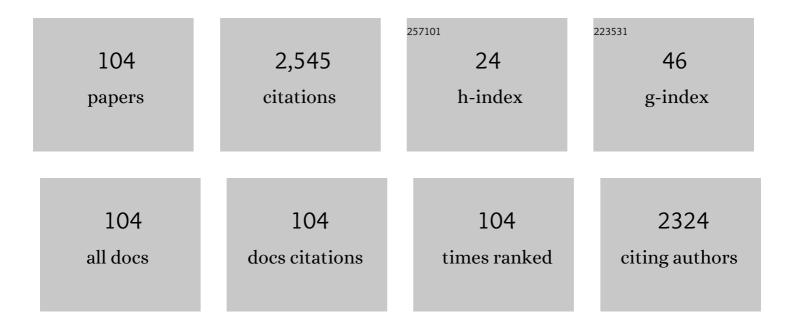
Xiao-Qiang Li

List of Publications by Year in descending order

Source: https://exaly.com/author-pdf/4402713/publications.pdf Version: 2024-02-01



#	Article	IF	CITATIONS
1	New Developments of Ti-Based Alloys for Biomedical Applications. Materials, 2014, 7, 1709-1800.	1.3	756
2	Ultrafine grained Ti-based composites with ultrahigh strength and ductility achieved by equiaxing microstructure. Materials & Design, 2015, 79, 1-5.	5.1	89
3	Fine-grained 93W–5.6Ni–1.4Fe heavy alloys with enhanced performance prepared by spark plasma sintering. Materials Science & Engineering A: Structural Materials: Properties, Microstructure and Processing, 2013, 573, 245-252.	2.6	76
4	Bulk WC–Al2O3 composites prepared by spark plasma sintering. International Journal of Refractory Metals and Hard Materials, 2012, 30, 51-56.	1.7	71
5	Biomedical TiNbZrTaSi alloys designed by d-electron alloy design theory. Materials and Design, 2015, 85, 7-13.	3.3	64
6	Effect of ultrasonic surface rolling at low temperatures on surface layer microstructure and properties of HIP Ti-6Al-4V alloy. Surface and Coatings Technology, 2017, 316, 75-84.	2.2	59
7	ZrO2 (3Y) toughened WC composites prepared by spark plasma sintering. Journal of Alloys and Compounds, 2013, 572, 62-67.	2.8	56
8	Wear mechanisms of WC–10Ni3Al carbide tool in dry turning of Ti6Al4V. International Journal of Refractory Metals and Hard Materials, 2015, 48, 272-285.	1.7	52
9	Fabrication, characterization, and mechanical properties of 93W–4.9Ni–2.1Fe/95W–2.8Ni–1.2Fe–1Al2 heavy alloy composites. Materials Science & Engineering A: Structural Materials: Properties, Microstructure and Processing, 2015, 636, 452-458.	2O3 2.6	50
10	Nucleation and growth mechanism of crystalline phase for fabrication of ultrafine-grained Ti66Nb13Cu8Ni6.8Al6.2 composites by spark plasma sintering and crystallization of amorphous phase. Materials Science & Engineering A: Structural Materials: Properties, Microstructure and Processing, 2010, 528, 486-493.	2.6	47
11	Non-isothermal and isothermal crystallization kinetics and their effect on microstructure of sintered and crystallized TiNbZrTaSi bulk alloys. Journal of Non-Crystalline Solids, 2016, 432, 440-452.	1.5	43
12	Densification and microstructure evolution during SPS consolidation process in W-Ni-Fe system. Transactions of Nonferrous Metals Society of China, 2011, 21, 493-501.	1.7	41
13	Microstructure and characterization of WC-2.8 wt% Al2O3-6.8 wt% ZrO2 composites produced by spark plasma sintering. Ceramics International, 2016, 42, 14182-14188.	2.3	40
14	Preparation and mechanical properties of WC-10 Ni3Al cemented carbides with plate-like triangular prismatic WC grains. Journal of Alloys and Compounds, 2012, 544, 134-140.	2.8	39
15	Microstructure and mechanical properties of fine-grained W–7Ni–3Fe heavy alloy by spark plasma sintering. Materials Science & Engineering A: Structural Materials: Properties, Microstructure and Processing, 2012, 551, 95-99.	2.6	39
16	93W–5.6Ni–1.4Fe heavy alloys with enhanced performance prepared by cyclic spark plasma sintering. Materials Science & Engineering A: Structural Materials: Properties, Microstructure and Processing, 2014, 599, 233-241.	2.6	39
17	Fabrication and properties of in situ reduced graphene oxideâ€ŧoughened zirconia composite ceramics. Journal of the American Ceramic Society, 2018, 101, 3498-3507.	1.9	38
18	Spark-Plasma Sintering of W-5.6Ni-1.4Fe Heavy Alloys: Densification and Grain Growth. Metallurgical and Materials Transactions A: Physical Metallurgy and Materials Science, 2013, 44, 923-933.	1.1	36

#	Article	IF	CITATIONS
19	The oxidation behavior of the WC–10wt.% Ni3Al composite fabricated by spark plasma sintering. Journal of Alloys and Compounds, 2015, 629, 148-154.	2.8	34
20	Effects of brazing temperature and testing temperature on the microstructure and shear strength of Î ³ -TiAl joints. Materials Science & Engineering A: Structural Materials: Properties, Microstructure and Processing, 2015, 634, 91-98.	2.6	33
21	Wear behavior of the micro-grooved texture on WC-Ni 3 Al cermet prepared by laser surface texturing. International Journal of Refractory Metals and Hard Materials, 2018, 72, 211-222.	1.7	29
22	Zirconia-toughened WC with/without VC and Cr3C2. Ceramics International, 2014, 40, 2011-2016.	2.3	28
23	Dynamic deformation behavior of 93W-5.6Ni-1.4Fe heavy alloy prepared by spark plasma sintering. International Journal of Refractory Metals and Hard Materials, 2016, 58, 117-124.	1.7	27
24	WC–Si3N4 composites prepared by two-step spark plasma sintering. International Journal of Refractory Metals and Hard Materials, 2015, 50, 133-139.	1.7	26
25	Highâ€ S trength AlCrFeCoNi High Entropy Alloys Fabricated by Using Metallic Glass Powder as Precursor. Advanced Engineering Materials, 2016, 18, 348-353.	1.6	26
26	In-situ elongated β-Si3N4 grains toughened WC composites prepared by one/two-step spark plasma sintering. Materials Science & Engineering A: Structural Materials: Properties, Microstructure and Processing, 2013, 561, 445-451.	2.6	25
27	Effect of Multi-Pass Ultrasonic Surface Rolling on the Mechanical and Fatigue Properties of HIP Ti-6Al-4V Alloy. Materials, 2017, 10, 133.	1.3	25
28	Effect of sintering temperature on phase constitution and mechanical properties of WC-1.0 wt% carbon nanotube composites. Ceramics International, 2018, 44, 164-169.	2.3	24
29	Effect of Heating Rate on Densification and Grain Growth During Spark Plasma Sintering of 93W-5.6Ni-1.4Fe Heavy Alloys. Metallurgical and Materials Transactions A: Physical Metallurgy and Materials Science, 2013, 44, 4323-4336.	1.1	23
30	Microstructure and properties of ultra-fine tungsten heavy alloys prepared by mechanical alloying and electric current activated sintering. Transactions of Nonferrous Metals Society of China, 2010, 20, 443-449.	1.7	22
31	Friction and Wear Behavior of 30CrMnSiA Steel at Elevated Temperatures. Journal of Materials Engineering and Performance, 2016, 25, 1407-1415.	1.2	21
32	Cr3C2 and VC doped WC–Si3N4 composites prepared by spark plasma sintering. International Journal of Refractory Metals and Hard Materials, 2013, 41, 540-546.	1.7	17
33	Machining performance of a grooved tool in dry machining Ti-6Al-4ÂV. International Journal of Advanced Manufacturing Technology, 2014, 73, 613-622.	1.5	17
34	In-situ elongated aluminium borate grains toughening WC- 1.87†wt % Al2O3- 4.13†wt % ZrO2 composite via spark plasma sintering. Ceramics International, 2019, 45, 19610-19616.	2.3	17
35	Microstructure and formation mechanism in a surface carburized tungsten heavy alloy. Journal of Alloys and Compounds, 2019, 787, 560-569.	2.8	17
36	Effect of shot peening on microstructure and contact fatigue crack growth mechanism of shaft steel. Materials Chemistry and Physics, 2021, 274, 125116.	2.0	17

#	Article	IF	CITATIONS
37	Experimental study on the laser-matter-plume interaction and its effects on ablation characteristics during nanosecond pulsed laser scanning ablation process. Optics Express, 2019, 27, 23204.	1.7	17
38	Effects of cutting parameters on dry cutting of aluminum bronze alloy. International Journal of Advanced Manufacturing Technology, 2014, 70, 669-678.	1.5	16
39	Synergistic effects of a combined surface modification technology on rolling contact fatigue behaviors of 20CrMoH steel under different contact stresses. International Journal of Fatigue, 2021, 153, 106487.	2.8	16
40	Bulk TiB2-Based Ceramic Composites with Improved Mechanical Property Using Fe–Ni–Ti–Al as a Sintering Aid. Materials, 2014, 7, 7105-7117.	1.3	14
41	Transitional/eutectic microstructure of Al 2 O 3 –ZrO 2 (Y 2 O 3) ceramics prepared by spark plasma sintering. Materials Letters, 2016, 175, 212-214.	1.3	14
42	Study on high temperature deformation behavior of WC-10Âwt %Ni3Al cemented carbide. Journal of Alloys and Compounds, 2020, 820, 153156.	2.8	14
43	Microstructure evolution and superelasticity of Ti-24Nb-xZr alloys fabricated by spark plasma sintering. Journal of Alloys and Compounds, 2020, 823, 153875.	2.8	14
44	Microstructure and magnetic properties of anisotropic Nd–Fe–B magnets prepared by spark plasma sintering and hot deformation. Transactions of Nonferrous Metals Society of China, 2014, 24, 3142-3151.	1.7	13
45	Microstructure evolution and mechanical properties of TiAl/GH536 joints vacuum brazed with Ti–Zr–Cu–Ni filler metal. Intermetallics, 2022, 142, 107468.	1.8	13
46	Abrasion wear behavior of WC–10Ni3Al cermet with plate-like triangular prismatic WC grains. Ceramics International, 2015, 41, 5147-5158.	2.3	12
47	The wear and fatigue behaviours of hollow head & sodium filled engine valve. Tribology International, 2018, 128, 75-88.	3.0	12
48	M3B2-type borides effect on the wide gap brazing of K417G alloy with mixed powder. Journal of Alloys and Compounds, 2020, 821, 153431.	2.8	12
49	Influence of particle size distribution on properties of SiC particles reinforced aluminum matrix composites with high SiC particle content. Journal of Composite Materials, 2016, 50, 1049-1058.	1.2	11
50	Brazeability evaluation of Ti-Zr-Cu-Ni-Co-Mo filler for vacuum brazing TiAl-based alloy. Transactions of Nonferrous Metals Society of China, 2019, 29, 754-763.	1.7	11
51	Influence of Effective Laser Energy on the Structure and Mechanical Properties of Laser Melting Deposited Ti6Al4V Alloy. Materials, 2020, 13, 962.	1.3	11
52	High temperature compressive properties and microstructure of WC-Ni3Al cermets prepared by spark plasma sintering. Vacuum, 2020, 175, 109281.	1.6	11
53	Fabrication of highly dissimilar TC4/steel joint with V/Cu composite transition layer by laser melting deposition. Journal of Alloys and Compounds, 2021, 862, 158319.	2.8	11
54	Effect of carburization on microstructure and rolling contact fatigue property of 95W–3.4Ni–1.6Fe heavy alloy. Transactions of Nonferrous Metals Society of China, 2016, 26, 3161-3169.	1.7	10

#	Article	IF	CITATIONS
55	Microstructure and shear strength of γ-TiAl/GH536 joints brazed with Tiâ^'Zrâ^'Cuâ^'Niâ^'Feâ^'Coâ^'Mo filler alloy. Transactions of Nonferrous Metals Society of China, 2020, 30, 2143-2155.	1.7	10
56	Microstructural evolution and mechanical properties of Alloy 718 fabricated by selective laser melting following different post-treatments. Rare Metals, 2021, 40, 3222.	3.6	10
57	Microstructure and Mechanical Properties of SPSed (Spark Plasma Sintered) Ti ₆₆ Nb ₁₃ Cu ₈ Ni _{6.8} Al _{6.2} Bulk Alloys with and without WC Addition. Materials Transactions, 2009, 50, 1720-1724.	0.4	9
58	Reciprocating wear behavior of WC–10Ni3Al cermet in contact with Ti6Al4V. Wear, 2014, 321, 16-24.	1.5	9
59	Comparison of TiAlâ€Based Intermetallics Joints Brazed with Amorphous and Crystalline Ti–Zr–Cu–Ni–Co–Mo Fillers. Advanced Engineering Materials, 2016, 18, 341-347.	1.6	9
60	Effect of Tempering Temperatures on Tensile Properties and Rotary Bending Fatigue Behaviors of 17Cr2Ni2MoVNb Steel. Metals, 2018, 8, 507.	1.0	9
61	Study on Microstructure and Mechanical Properties of WC-10Ni3Al Cemented Carbide Prepared by Different Ball-Milling Suspension. Materials, 2019, 12, 2224.	1.3	9
62	The influence of sintering temperature and pressure on microstructure and mechanical properties of carbonyl iron powder materials fabricated by electric current activated sintering. Vacuum, 2017, 137, 137-147.	1.6	8
63	Dynamic mechanical behavior of 93W–4.9Ni–2.1Fe/95W–2.8Ni–1.2Fe–1Al2O3 heavy alloy composite Materials Science & Engineering A: Structural Materials: Properties, Microstructure and Processing, 2018, 729, 349-356.	2.6	8
64	Microstructure and mechanical properties of TiAl/Ni-based superalloy joints vacuum brazed with Ti–Zr–Fe–Cu–Ni–Co–Mo filler metal. Rare Metals, 2021, 40, 2134-2142.	3.6	8
65	Effects of Al2O3–ZrO2 content on the densification, microstructure, and mechanical properties of cemented tungsten carbides. Materials Chemistry and Physics, 2022, 276, 125330.	2.0	8
66	Microstructures and fatigue behaviors of 25CrNi2MoV steel under electropulsing-assisted ultrasonic surface rolling. International Journal of Fatigue, 2022, 158, 106733.	2.8	8
67	Preparation of SiCp/Al composite–bismuthate glass material and its application in mirror blanks. RSC Advances, 2015, 5, 52167-52173.	1.7	7
68	Effect of Pulsed Magnetic Field on Spark Plasma Sintering of Iron-Based Powders. Materials Transactions, 2010, 51, 1308-1312.	0.4	6
69	Spark Plasma Sintered Hydroxyapatite/Multiwalled Carbon Nanotube Composites With Preferred Crystal Orientation. Advanced Engineering Materials, 2010, 12, 1161-1165.	1.6	6
70	SPS densification behavior of W-5.6Ni-1.4Fe heavy alloy powders. Rare Metals, 2011, 30, 581-587.	3.6	6
71	Fabrication of Ultrafine-Grained Ti ₆₆ Nb ₁₈ Cu _{6.4} Ni _{6.1Composites with High Strength and Distinct Plasticity by Spark Plasma Sintering and Crystallization of Amorphous Phase, Materials Transactions, 2012, 53, 531-536.}	t:Al <su 0.4</su 	ıb>3.5<
72	Properties of SiC _p /6061-Al metal matrix composites prepared by infiltrating molten aluminum into ternary packing of SiC preforms. Journal of Composite Materials, 2015, 49, 3609-3619.	1.2	6

#	Article	IF	CITATIONS
73	Surface modification layer of Ti–6Al–4V produced by surface rolling and thermal oxidation. Surface Innovations, 2017, 5, 232-242.	1.4	6
74	Deformation induced precipitation of MgZn2-type laves phase in Ti-Fe-Co alloy. Journal of Alloys and Compounds, 2019, 778, 795-802.	2.8	6
75	Microstructure and tribological properties of carburized 95W–3.5Ni–1.0Fe–0.5Co heavy alloy. Rare Metals, 2019, 38, 165-172.	3.6	6
76	Fabrication of in situ elongated β-Sialon grains bonded to tungsten carbide via two-step spark plasma sintering. Ceramics International, 2021, 47, 27324-27333.	2.3	6
77	Corrosion Behavior of WC–10 wt % Ni3Al Composite in Acidic Media. Journal of Superhard Materials, 2019, 41, 345-354.	0.5	5
78	A comparison of wear behaviour of heat-resistant steel engine valves and TiAl engine valves. Proceedings of the Institution of Mechanical Engineers, Part J: Journal of Engineering Tribology, 2020, 234, 1549-1562.	1.0	5
79	Wide-Gap Brazing of K417G Alloy Assisted by In Situ Precipitation of M3B2 Boride Particles. Materials, 2020, 13, 3140.	1.3	5
80	Ultrafine porous boron nitride nanofiberâ€ŧoughened WC composites. International Journal of Applied Ceramic Technology, 2020, 17, 941-948.	1.1	5
81	Concurrent Hardening and Toughening of a Tungsten Heavy Alloy via a Novel Carburizing Cyclic Heat Treatment. Advanced Engineering Materials, 2021, 23, 2001283.	1.6	5
82	Microstructure and oxidation resistance of CoNiCrAlY coating manufactured by laser powder bed fusion. Surface and Coatings Technology, 2021, 427, 127846.	2.2	5
83	Examination of Electrical Conduction of Carbonyl Iron Powder Compacts. Materials Transactions, 2015, 56, 696-702.	0.4	4
84	Serrated Flow Behavior of Titaniumâ€Based Composites with Different In Situ TiC Contents. Advanced Engineering Materials, 2015, 17, 1383-1390.	1.6	4
85	Design and operation of a new multifunctional wear apparatus for engine valve train components. Proceedings of the Institution of Mechanical Engineers, Part J: Journal of Engineering Tribology, 2018, 232, 259-276.	1.0	4
86	Mechanical Properties of WC-Si3N4 Composites With Ultrafine Porous Boron Nitride Nanofiber Additive. Frontiers in Materials, 2021, 8, .	1.2	4
87	Reutilization of a reflected laser beam as an effective approach for machining metallic materials with low laser absorptivity. Optics Express, 2019, 27, 12048.	1.7	4
88	Effects of Alloy Composition on Microstructure and Mechanical Properties of Iron-Based Materials Fabricated by Ball Milling and Spark Plasma Sintering. Metallurgical and Materials Transactions A: Physical Metallurgy and Materials Science, 2015, 46, 476-487.	1.1	3
89	Optimization of Friction Welding Process Parameters for 42Cr9Si2 Hollow Head and Sodium Filled Engine Valve and Valve Performance Evaluation. Materials, 2019, 12, 1123.	1.3	3
90	Effect of filler metal on the microstructural evolution and mechanical properties of wide gap brazed K417G superalloy joints. Vacuum, 2021, 184, 109967.	1.6	3

#	Article	IF	CITATIONS
91	Research on microstructural and property evolution in laser cladded HAZ. Surface Engineering, 2021, 37, 1514-1522.	1.1	3
92	Effect of Shot Peening on Microstructures and Highâ€Temperature Tribological Properties of 4Cr9Si2 Valve Steel. Steel Research International, 0, , 2100250.	1.0	3
93	Interfacial characterization and mechanical properties of additively manufactured IN718/CoNiCrAlY laminate. Materials Science & Engineering A: Structural Materials: Properties, Microstructure and Processing, 2022, 850, 143578.	2.6	3
94	Effect of Minor Alloying Substitution on Glass-Forming Ability and Crystallization Behavior of a Ni ₅₇ Zr ₂₂ X ₈ Nb ₈ Al& (X = Ti, Cu) Alloy Synthesized by Mechanical Alloying. Materials Transactions, 2013, 54, 1844-1850.	kltjsub>	;5
95	Sinter-hardening with concurrent improved plasticity in iron alloys induced by spark plasma sintering. Journal of Materials Research, 2014, 29, 981-988.	1.2	2
96	Wear behavior and mechanism of a sliding pair of 0. 1C-3Cr-2W-V nitrided steel rubbing against an aluminum bronze alloy. Journal of Iron and Steel Research International, 2016, 23, 281-288.	1.4	2
97	Study on Strain Rate–Dependent Deformation Mechanism of WC–10 wt% Ni 3 Al Cemented Carbide by Micropillar Compression. Advanced Engineering Materials, 2020, 22, 1900953.	1.6	2
98	Drop Tower Experiment to Study the Effect of Microgravity on Friction Behavior: Experimental Set-up and Preliminary Results. Microgravity Science and Technology, 2020, 32, 1095-1104.	0.7	2
99	Evolution of the Fretting Wear Damage of a Complex Phase Compound Layer for a Nitrided High-Carbon High-Chromium Steel. Metals, 2020, 10, 1391.	1.0	2
100	Study on High Temperature Friction and Wear Characteristics of 4Cr9Si2 Valve Steel. Mechanisms and Machine Science, 2018, , 1535-1546.	0.3	1
101	Preparation and Anodizing of SiCp/Al Composites with Relatively High Fraction of SiCp. Scanning, 2018, 2018, 1-13.	0.7	1
102	Brazing Oxide Dispersion-Strengthened Fe-Based Steels with a Cu-Based Filler Metal. Journal of Materials Engineering and Performance, 2019, 28, 2184-2191.	1.2	1
103	The ΣÂ=Â2 and ΣÂ=Â13a grain boundary distributions in cemented tungsten carbides with/without metallic binders. Materials Characterization, 2021, 173, 110872.	1.9	1
104	Preparation of in situ and ex situ reinforced Fe-10Cr-1Cu-1Ni-1Mo-2C containing NbC particles by milling and hot pressing. International Journal of Minerals, Metallurgy and Materials, 2015, 22, 157-166.	2.4	0